Articles

Chinese Science Bulletin

Chemical Biology

April 2010 Vol.55 No.11: 1013−1019
doi: 10.1007/s11434-010-0046-1

The effects of gold nanoparticles on the proliferation, differentiation, and mineralization function of MC3T3-E1 cells *in vitro*

LIU DanDan[1,2], ZHANG JinChao[1*], YI ChangQing[2,3] & YANG MengSu[2,3*]

[1] *Chemical Biology Laboratory, College of Chemistry and Environmental Science , Hebei University, Baoding 071002, China;*
[2] *Key Laboratory of Biochip Research, Shenzhen Research Institute of City University of Hong Kong, Shenzhen 518057, China;*
[3] *Department of Biology and Chemistry, City University of Hong Kong, Hong Kong, China*

Received March 16, 2009; accepted September 22, 2009

This study has investigated the effects of gold nanoparticles (Au NPs) on the proliferation, differentiation, and mineralization of a murine preosteoblast cell line MC3T3-E1 *in vitro*. The results show that Au NPs with diameters of both 20 and 40 nm promoted the proliferation, differentiation, and mineralization of MC3T3-E1 cells in a time- and dose-dependent manner at the concentrations of 1.5×10^{-5}, 3.0×10^{-5}, and 1.5×10^{-4} μmol/L. The reverse transcriptase polymerase chain reaction (RT-PCR) indicates that the expressions of runt-related transcription factor 2 (*Runx2*), bone morphogenetic protein 2 (*BMP-2*), alkaline phosphatase (*ALP*), and osteocalcin (*OCN*) genes increased after the 20 and 40 nm Au NP treatments, and the expression levels were higher than those of the NaF group. The above results suggest that Au NPs have the potential to promote the osteogenic differentiation and mineralization of MC3T3-E1 cells and the particle size plays a significant role in the process. *Runx2*, *BMP-2*, *ALP*, and *OCN* genes may interact with each other, further stimulating the osteogenic differentiation of MC3T3-E1 cells.

gold nanoparticles, proliferation, osteogenic differentiation, mineralization

Citation: Liu D D, Zhang J C, Yi C Q, et al. The effects of gold nanoparticles on the proliferation, differentiation, and mineralization function of MC3T3-E1 cells *in vitro*. Chinese Sci Bull, 2010, 55: 1013−1019, doi: 10.1007/s11434-010-0046-1

The recent advances in nanotechnology show the prospect for the nanotechnology-based biomaterials. Nanoparticles due to their special physical properties, are widely applied in the fields, such as diagnostics, drug delivery, tissue engineering, and sensing. The advanced nanotechnology enhances nano-based consumer products [1,2]. Gold nanoparticles (Au NPs), also called gold colloids, have some unique physical properties and biocompatible features as well as unique surface properties including surface topography, surface chemistry, and surface energy [3]. The wide applications of gold nanoparticles in biological fields (such as biosensor [4,5], drug vector [6], and cancer diagnosis and gene therapy [7]) prove their multi-property features.

While benefits of nanotechnology are widely publicized, the discussion on the potential effects of their widespread use in humans is just beginning to emerge [8,9]. It has been shown that nanoparticles can enter the human body through several ports. Many nanoparticles can enter the lungs where it is possible for them to transfer to other vital organs rapidly through the blood stream [10]. These nanoparticles include silicon nanoparticles, iron oxide nanoparticles, albumin nanoparticles and so on. It has been reported that gold nanoparticles are present in various organ systems including the blood, liver, spleen, kidney, testis, thymus, heart, lung, brain and marrow [10,11].

In a human's whole life, the bone is a mineralized tissue which contains two distinct types of cells: osteoblasts and osteoclasts. Osteoblasts stem from bone marrow stromal cells and synthesize and mineralize the collagenous extracellular matrix of the bone [12], while osteoclasts stem from bone marrow hematopoietic cells, which take part in resorbing old bone. The abnormality in the balance between osteoblast and osteoclast activities results in skeletal disorder such as osteopetrosis, osteoporosis, and inflammatory

*Corresponding authors (email: jczhang6970@yahoo.com.cn; bhmyang@cityu.edu.hk)

bone erosion, all of which threaten the human health [13]. Although Au NPs have many applications in biological fields, it is still unclear whether Au NPs can affect the structure and function of the bone.

The bone is a nanocomposite that consists of a protein based soft hydrogel template and hard inorganic components (hydroxyapatite, HA). Specifically, 70% of the bone matrix is composed of nanocrystalline HA which is typically 10–50 nm long and 10 nm thick [14]. So far, the effects of Au NPs on the proliferation, differentiation, and mineralization of a murine preosteoblast cell line MC3T3-E1 *in vitro* have not been reported. Therefore, we investigated the biological effects of Au NPs with diameters of both 20 and 40 nm on the proliferation, differentiation and mineralization of a murine preosteoblast cell line MC3T3-E1 in this paper.

1 Materials and methods

1.1 Gold nanoparticles (Au NP)

The colloidal gold particles (obtained with a Phillips Tecnai 12 instrument) were measured by transmission electron microscopy (TEM) and energy dispersive X-ray (EDX) methods. The size of the particles was homogenous with diameters of 20 and 40 nm, which were similar to the theoretical size. The preparation of colloidal gold had a polydispersity and did not have sedimentation phenomenon observed from the images of TEM (Figure 1(a) and (b)). The results of EDX measurement indicate that the primary elements of the colloidal gold were Au (Figure 2(a) and (b)).

1.2 Culture of murine preosteoblast MC3T3-E1 cells

Mouse calvarial preosteoblasts (MC3T3-E1) were purchased from ATCC (Manassas, VA, USA) and cultured in alpha minimum essential medium (α-MEM) supplemented with 10% (v/v) fatal bovine serum (FBS), 100 U/mL penicillin and 100 U/mL streptomycin. Incubation was conducted in a CO_2 incubator (5% CO_2, 95% air) (Sanyo, Model MCO-18AIC) at 37°C. The cells were subcultured every 3 d in the presence of 0.25% (w/v) trypsin plus 0.02% (w/v) ethylenediaminetetraacetic acid tetrasodium salts solution (EDTA) (Gibico).

1.3 Assay for proliferation

The proliferation of MC3T3-E1 cells was measured according to the colorimetric 3-(4,5-dimethylthiazol-2-yl)-2, 5-diphenyltetrazolium bromide (MTT) method as described

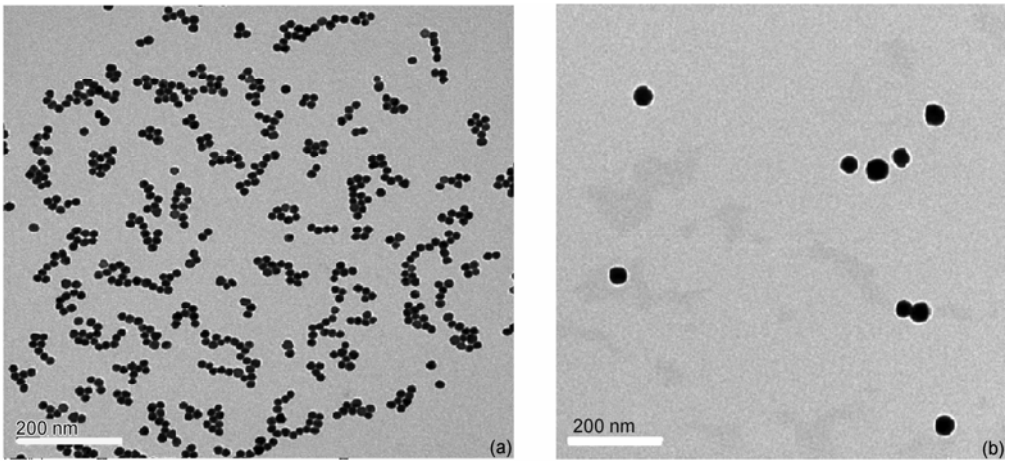

Figure 1 TEM of the gold nanoparticles with diameters of 20 (a) and 40 nm (b).

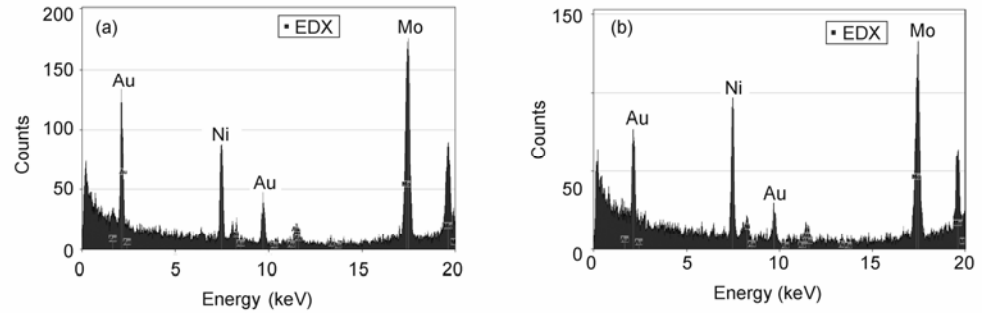

Figure 2 EDX of the gold nanoparticles with diameters of 20 (a) and 40 nm (b).

previously [15]. In brief, MC3T3-E1 cells were plated on 96-well plates (5000 cells/well). After preincubation, fresh media containing Au NPs were added. Cells without Au NPs treatment were used as negative control, and wells without cells were set as blanks. After treatment, 20 μL of MTT (5.0 mg/mL, Sigma, USA) was added and incubated for another 4 h at 37°C. Then, the supernatant was removed and dimethyl sulfoxide (DMSO) was added, and the absorbance at 570 nm was recorded on a microplate spectrophotometer (Bio-Rad Model 680, USA). The proliferation rate (%) was calculated according to the formula: $(A_{\text{sample}} - A_{\text{control}})/A_{\text{control}} \times 100\%$.

1.4 Assay for alkaline phosphatase (ALP) activity

MC3T3-E1 cells were seeded in 24-well plates (2×10^4 cells/well) containing α-MEM medium plus 10% FBS. After 24 h, the culture medium was changed to α-MEM+10% FBS medium containing osteogenic induced supplement (10 mmol/L disodium β-glycerophosphate (β-GP) (BBI), 0.15 mmol/L ascorbic acid (Sigma) and 10^{-8} mol/L dexamethasone (Sigma)) [16]. Simultaneously, NaH_2PO_4 was added to set the final phosphate concentration to be 3.0 mmol/L. After 7 and 14 d cultivation with Au NPs, the plates were washed twice with ice-cold D-Hank's and lysed by two cycles of freezing and thawing. Aliquots of supernatants were subjected to alkaline phosphatase activity and protein content measurement by an alkaline phosphatase activity kit (Nanjing Jiancheng Biological Engineering Institute, China) and a micro-Bradford assay kit (Beyotime Biotechnology, China). All results were normalized by protein content.

1.5 Assay for mineralized matrix formation

MC3T3-E1 cells (2×10^4 cells/well) were seeded in 24-well tissue culture plates and cultured overnight at 37°C in a 5% CO_2 humidified incubator. The medium was then changed to differentiation medium containing 10 mmol/L β-glycerophosphate (BBI) and 50 μg/mL ascorbic acid (Sigma) in the presence of 1.5×10^{-5}, 3.0×10^{-5}, and 1.5×10^{-4} μmol/L of Au NPs for 8 d, and then transferred to a medium containing 3.0 mmol/L NaH_2PO_4 for an additional 8 and 12 d [17]. The formation of mineralized matrix nodules was determined by alizarin red S (Sigma) staining. Briefly, the cells were fixed in 70% ethanol for 1 h at room temperature. The fixed cells were washed with D-Hank's and stained with 1% (w/v) alizarin red S at pH 4.2 for 30 min at room temperature. Quantitative analysis of alizarin red S staining was performed by elution with 10% (w/v) cetylpyridium chloride (Sigma) for 10 min at room temperature and the absorbance was measured at 570 nm [18]. Results were expressed as the mineralized promotion rate (%).

1.6 Reverse transcriptase polymerase chain reaction (RT-PCR)

Total RNA was prepared using Trizol (Invitrogen) according to the manufacturer's protocol after treated with Au NPs for 7 d, and the concentration was measured by a spectrophotometer (Eppendorf Biophotometer, Germany). First-strand cDNAs were obtained according to the TaKaRa protocol (TaKaRa, Tokyo). PCR was performed by using 1 μL of the RT products, *Go Taq* polymerase (TaKaRa), and the following primers. In all, 40 cycles of amplification as indicated in Table 1 were carried out in the following conditions for each cycle: denaturing at 94°C for 1 min, annealing at 56°C for 30 s, and extension at 72°C for 30 s. *Glyceraldehyde-3-phosphate dehydrogenase* (*GAPDH*) was used as an internal control. The list of gene specific primers used is shown in Table 1.

1.7 Statistical analysis

Data were collected from at least three separate experiments and expressed as means ± standard deviation (SD). The statistical differences were analyzed by a paired Student's *t*-test. *P* values less than 0.05 were considered to indicate statistical differences.

2 Results

2.1 Effects of Au NPs on the proliferation of MC3T3-E1 cells

As shown in Figure 3, Au NPs with a diameter of 20 nm promoted the proliferation of MC3T3-E1 cells in a time- and dose-dependent manner, and Au NPs with a diameter of 40 nm promoted the proliferation of MC3T3-E1 cells in a dose-dependent manner at the concentrations of 1.5×10^{-5}, 3.0×10^{-5}, and 1.5×10^{-4} μmol/L.

2.2 Effects of Au NPs on the differentiation of MC3T3-E1 cells

As shown in Figure 4, Au NPs with diameters of both 20

Table 1 RT-PCR primers

Gene symbol	Forward primer (5′→3′)	Reverse primer (5′→3′)
Runx2	TTCTCCAACCCACGAATGCAC	CAGGTACGTGTGGTAGTGAGT
BMP-2	TGGCCCATTTAGAGGAGAACC	AGGCATGATAGCCCGGAGG
ALP	GTTGCCAAGCTGGGAAGAACAC	CCCACCCCGCTATTCAAAC
OCN	GAACAGACTCCGGCGCTA	AGGGAGGATCAAGTCCCG
GAPDH	GACTTCAACAGCAACTCCCAC	TCCACCACCCTGTTGCTGTA

and 40 nm promoted the osteogenic differentiation of MC3T3-E1 cells in a time- and dose-dependent manner at the concentrations of 1.5×10^{-5}, 3.0×10^{-5}, and 1.5×10^{-4} μmol/L for 7 and 14 d.

2.3 Effects of Au NPs on the formation of mineralized matrix nodules

As shown in Figure 5 (a) and (b), Au NPs with diameters of both 20 and 40 nm promoted the mineralization function of MC3T3-E1 cells in a dose-dependent manner at the concentrations of 1.5×10^{-5}, 3.0×10^{-5} and 1.5×10^{-4} μmol/L, and the promotion rate of 20 nm Au NPs is higher than that of 40 nm Au NPs. Moreover, the experimental results are in accordance with morphological observations (Figure 6).

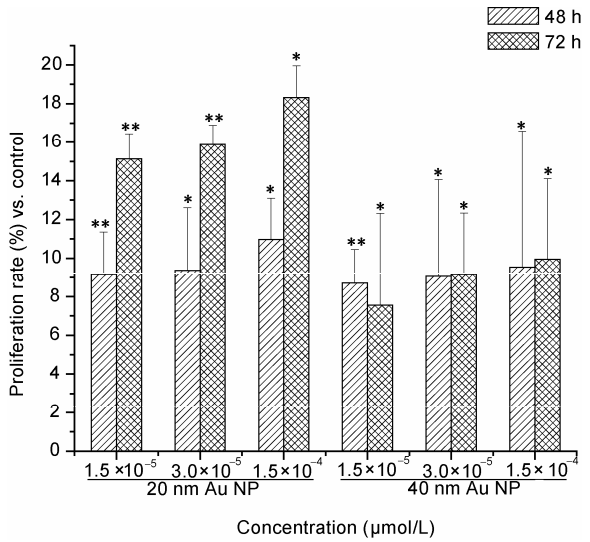

Figure 3 Time- and dose-dependent effects of Au NPs with diameters of both 20 and 40 nm on the proliferation of MC3T3-E1 cells (*P < 0.05, **P<0.01 compared with the control group, n = 6).

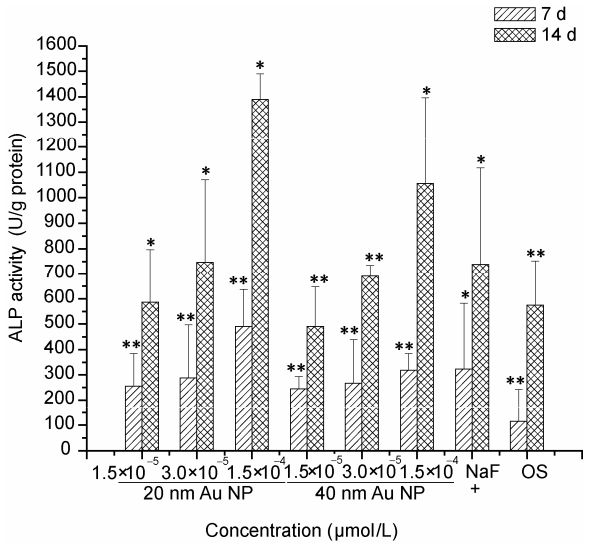

Figure 4 Time- and dose-dependent effects of Au NPs of with diameters of both 20 and 40 nm on the ALP activity of MC3T3-E1 cells (*P < 0.05, **P<0.01 compared with the control group, n = 6).

2.4 RT-PCR analysis of gene expression

As shown in Figure 7, Au NPs with diameters of both 20 and 40 nm promoted the expressions of *Runx2*, *BMP-2*, *ALP* and *OCN* genes. Moreover, their expression level was higher than that of the NaF group.

3 Discussion

The murine preosteoblast MC3T3-E1 cell line is an excellent cell differentiation model that stimulates the events of early osteoblastogenesis. MC3T3-E1 cells require only serum and ascorbic acid (AA) to express a fully differentiated phenotype [17]. Therefore MC3T3-E1 cell line may provide a useful system for the study of the regulation signals in relation to the different stages from proliferation to mineralization *in vitro*. In our study, we found that Au NPs with diameters of both 20 and 40 nm promoted the proliferation of MC3T3-E1 cells in a time- and dose-dependent manner at the concentrations of 1.5×10^{-5}, 3.0×10^{-5} and 1.5×10^{-4} μmol/L. Our results indicate that Au NPs did not have acute cytotoxic effect on MC3T3-E1 cells. ALP activity is an early marker of osteoblastic activity, i.e., bone turnover and bone remodeling. Its level in serum was increased during bone healing after fracture [19,20]. Our experimental results indicate that Au NPs of with diameters both 20 and 40 nm also promoted the osteogenic differentiation of MC3T3-E1 cells in a time- and dose-dependent manner at the concentrations of 1.5×10^{-5}, 3.0×10^{-5} and 1.5×10^{-4} μmol/L for 7 and 14 d. Moreover, ALP activity of MC3T3-E1 cells treated with 20 nm Au NPs was higher than that treated with 40 nm Au NPs for 7 or 14 d at the same concentration. An essential sign for the osteogenic differentiation of MC3T3-E1 is bone matrix maturation and mineralization. The appearance of ALP activity is an early phenotypic marker for osteogenic differentiation and mineralized nodule formation is a phenotypic marker for the last stage of mature osteoblasts. Two to three weeks later osteoblast node was formed and reached a peak when osteoblast was mineralized [21–23]. In this paper, we found that Au NPs with diameters of both 20 nm and 40 nm promoted the mineralization function of MC3T3-E1 cells in a dose-dependent manner at the concentrations of 1.5×10^{-5}, 3.0×10^{-5} and 1.5×10^{-4} μmol/L. Moreover, the promotion rate of 20 Au NPs is higher than that of 40 nm Au NPs. Many researchers have reported that nanoscale particles and nanoparticle-modified surfaces could promote the minerali zation [24–27]. Bone consists mainly of collagen proteins and hydroxyapatite, where both the size and the orientation of the hydroxyapatite crystals (10–50 nm length and 10 nm in width) are dictated specifically by the collagen template. The precise structural relationship between the collagen and hydroxyapatite is critical to the bone's resilience and strength [28]. Because nanomaterials

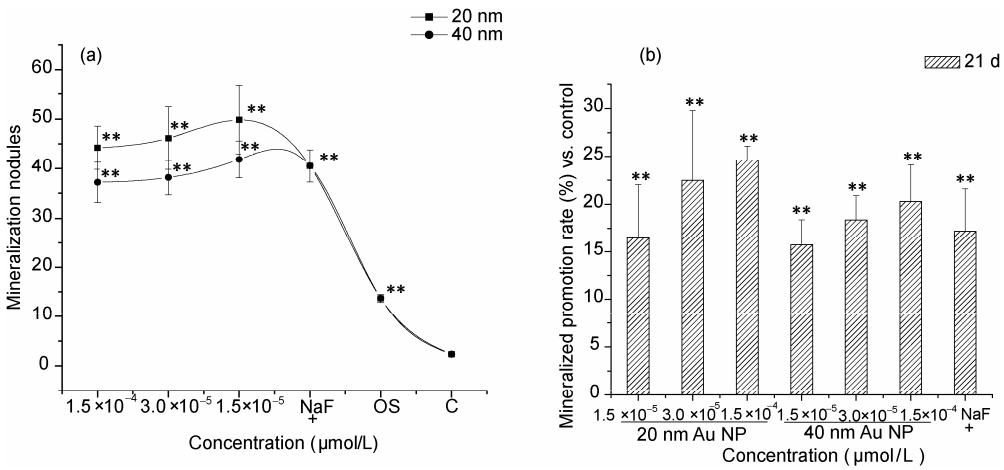

Figure 5 Effects of Au NPs on the mineralized nodule formation of MC3T3-E1 cells. (a) The number of alizarin red S staining nodules; (b) mineralization quantitated by elution of alizarin red S from stained mineral deposits (*$P < 0.05$, **$P<0.01$ compared with the control group, $n = 6$).

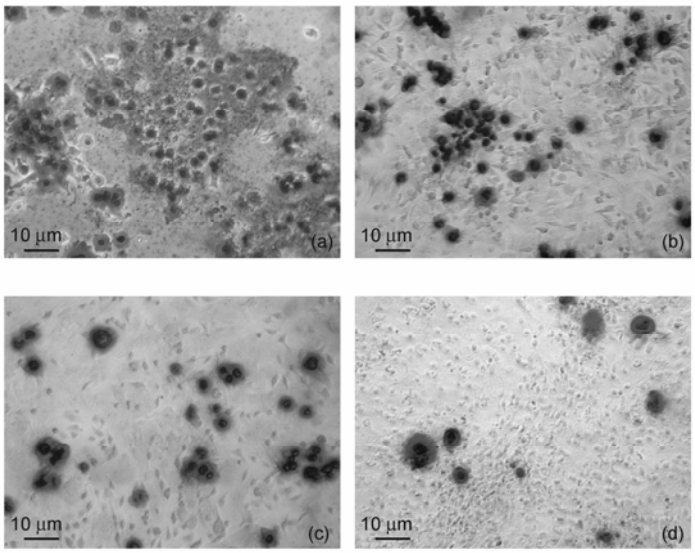

Figure 6 The mineralized nodule formation in the presence of Au NPs stained by alizarin red S. (a) Cells treated with 1.5×10^{-4} μmol/L 20 nm Au NPs; (b) cells treated with 1.5×10^{-4} μmol/L 40 nm Au NPs; (c) cells treated with 1.0×10^{-6} mol/L NaF; (d) cells without Au NPs as control. Original magnification = 100.

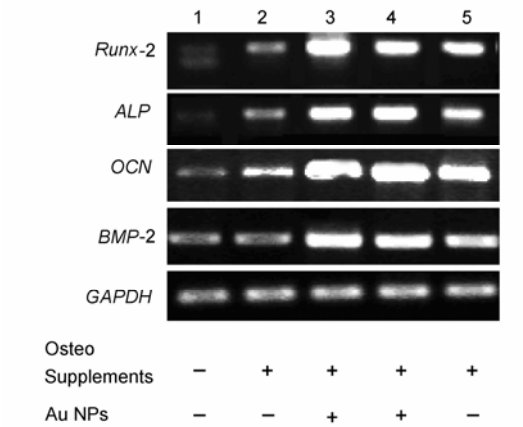

Figure 7 Agarose gel (1.2%) electrophoresis for RT-PCR products. 1: control group without osteogenic induce supplement (OS) and Au NPs; 2: cells treated with OS; 3: cells treated with 20 nm Au NP and OS; 4: cells treated with 40 nm Au NPs and OS; 5: cells treated with 1.0×10^{-6} mol/L NaF and OS as positive control.

have dimensions similar to hydroxyapatite crystals and collagen fibres found in the bone [29], we hypothesized that Au NPs is just like a crystal nucleus, which is similar to the hydroxyapatite crystal in size. Therefore, Au NPs stimulated cells' proliferation, differentiation and mineralization, around which calcium deposited.

A large number of genes which have been associated with bone cells are known to be specifically required for osteoblast differentiation, such as *Runx2*, *BMP-2*, *ALP* and *OCN* [30]. Runt-related transcription factor 2 (*Runx2*) is a master regulator of osteogenic gene expression and osteoblast differentiation. *Runx2* knockout mice exhibited no bone tissues or osteoblasts, indicating that osteoblast differentiation is completely blocked in the absence of *Runx2* [31]. Consistent with these observations, transgenic mice overexpressing the dominant negative form of *Runx2* exhibited an osteopenic phenotype and reduced bone formation

[30]. *Runx2*-expressing cells shared several properties with primary osteoblasts including a requirement for ascorbic acid-dependent extra-cellular matrices (ECM) synthesis for optimal differentiation and a clear temporal sequence in the expression of differentiation markers [32]. Alkaline phosphatase (ALP) is considered to play an important role in processes leading to mineral formation in tissues like bone, cartilage tooth root cementum, and dentin [33]. OCN is the most abundant noncollagenous components of the bone ECM; their expression levels can suggest the degree of ECM mineralization [34], while the mineralization is an indication of bone cell differentiation. Bone morphogenetic protein (BMP-2) which is a potent osteogenic protein required for osteoblast differentiation and bone formation, can induce low level expression of osteoblast marker genes such as osteocalcin (*OCN*) and alkaline phosphatase (*ALP*) in calvarial cells from *Cbfa1*$^{-/-}$ animals, although these cells are not able to form a mineralized matrix [35]. At molecular level, our results indicate there was significant higher expression level of *Runx2*, *BMP-2*, *ALP* and *OCN* treatment with Au NPs in MC3T3-E1 cells. The order of expressions is 20 nm >40 nm >NaF. The expression of *Runx2* induced *ALP* activity at early stages followed by *OCN* and mineralization. Combined with the ARS stained results, the results suggest that higher expression of *OCN* stimulates mineralization in MC3T3-E1 cells. It is well known that *BMP-2* induces osteogenic differentiation of MC3T3-E1 by simulating downstream osteogenic master transcription factor Runx2, which in turn works sequentially, and together with *BMP-2* to induce the expressions of bone marker genes that represent transdifferentiation [36]. In view of these findings, we deduced that *BMP-2* may be able to compliment Runx2 dependent gene expression to stimulate osteoblast differentiation. Then *Runx2* gene induced *ALP* at early time followed by *OCN* and mineralization [32]. At the same time, *BMP-2* induced expressions of *ALP* and *OCN* genes to stimulate the osteogenic differentiation of MC3T3-E1 cells. In addition we found that expressions of 20 nm groups were higher than those of the 40 nm groups. Reports in the literature demonstrated that the influence of nanoparticle size on bone cell function [37–40]. It has been reported that gold, silver, alumina and titania nanoparticles mediated cellular response is size-dependent [41,42]. The present study demonstrates, for the first time, that nanometer Au promoted the viability and osteogenic differentiation of MC3T3-E1 cells. Furthermore, because the synthetic method, chemistry and material phase of Au NPs were similar in the present study, the results of proliferation, osteogenic differentiation and mineralization of MC3T3-E1 were dependent mainly on the size of Au NPs. It was suggested that the diameter of the Au NPs may play an important role in increasing viability and ALP activity. The mechanism involved in the promoted osteogenic differentiation and mineralization of MC3T3-E1 cells after exposure to Au NPs remains to be further studied.

4 Conclusions

In summary, our experimental results demonstrate that Au NPs do not have acute cytotoxic effect on MC3T3-E1 cells and have the potential to promote the osteogenic differentiation and mineralization. Moreover, the size of particles has a significant influence on the proliferation, osteogenic differentiation, and mineralization of MC3T3-E1 cells. RT-PCR results indicated that the expressions of *Runx2*, *BMP-2*, *ALP* and *OCN* genes were increased after the cells were treated with 20 and 40 nm Au NPs. The diameter of the Au NPs may play an important role in increasing viability and ALP activity. Further studies on the molecular mechanisms of such effects are needed to provide a better understanding on the impact of Au NPs on biological systems and important information for future safe applications of Au NPs and the design of biocompatible nanomaterials.

This work was supported by the Key Laboratory Funding Scheme of Shenzhen Municipal Government, the AOE about MERIT project from University Grant Committee of Hong Kong (*Grant No. AOE/P-04/2004*) *and the Natural Science Foundation of Hebei Province* (*Grant No. B2009000161*).

1 Mazzola L. Commercializing nanotechnology. Nat Biotechnol, 2003, 21: 1137–1143
2 Paull R, Wolfe J, Hebert P, et al. Investing in nanotechnology. Nat Biotechnol, 2003, 21: 1144–1147
3 Marie-Christine D, Didier A. Gold nanoparticles: Assembly, supramolecular chemistry, quantum-size-related properties, and applications toward biology, catalysis, and nanotechnology. Chem Rev, 2004, 104: 293–346
4 Frederix F, Friedt J M, Choi K H, et al. Biosensing based on light absorption of nanoscaled gold and silver particles. Anal Chem, 2003, 75: 6894–6900
5 Liu T, Tang J A, Zhao H Q, et al. Particle size effect of the DNA sensor amplified with gold nanoparticles. Langmuir, 2002, 18: 5624–5626
6 Paciotti G F, Myer L, Weinreich D, et al. Colloidal gold: A novel nanoparticle vector for tumor directed drug delivery. Drug Delivery, 2004, 11: 169–183
7 Yang N, Sun W H. Gene gun and other non-viral approaches for cancer gene therapy. Nat Med, 1995, 1: 481–483
8 Luther W. 2nd ed: Industrial application of nanomaterials – chances and risks. Future Technologies, 2004, 54: 1–112
9 Siegrist M, Wiek A, Helland A, et al. Risks and nanotechnology: The public is more concerned than experts and industry. Nat Nanotech, 2007, 2: 67–68
10 De Jong W H, Hagens W I, Krystek P, et al. Particle size-dependent organ distribution of gold nanoparticles after intravenous administration. Biomaterials, 2008, 29: 1912–1919
11 Grislain L, Couvreur P, Lenaerts V, et al. Pharmacokinetics and distribution of a biodegradable drug-carrier. Int J Pharm, 1983, 15: 335–345
12 Pittenger M F, Mackay A M, Beck S C, et al. Multilineage potential of adult human mesenchymal stem cell. Science, 1999, 284: 143–147
13 Karsenty G, Wagner E F. Reaching a genetic and molecular understanding of skeletal development. Dev Cell, 2002, 2: 389–406
14 Kaplan F S, Hayes W C, Keaveny T M, et al. In: Simon S R, ed. Orthopedic Basic Science. Rosemont: American Academy of Orthopaedic Surgeons, 1994. 127–185

15 Carmichael J, Degraff W G, Gazdar A F, et al. Evaluation of a tetrazolium-based semiautomated colorimetric assay: Assessment of chemosensitivity testing. Cancer Res, 1987, 47: 936–942
16 Zhao Y, Zou B, Shi Z Y, et al. The effect of 3-hydroxybutyrate on the in vitro differentiation of murine osteoblast MC3T3-E1 and in vivo bone formation in ovariectomized rats. Biomaterials, 2007, 28: 3063–3073
17 Wang D, Christensen K, Chawla K, et al. Isolation and characterization of MC3T3-E1 preosteoblast subclones with distinct in vitro and in vivo differentiation/mineralization potential. Bone Miner Res, 1999, 14: 893–903
18 Gori F, Divieti P, Demay M. Cloning and characterization of a novel WD-40 repeat protein that dramatically accelerates osteoblastic differentiation. J Biol Chem, 2001, 276: 46515–46522
19 Obrant K J, Ivaska K K, Gerdhem P, et al. Biochemical markers of bone turnover are influenced by recently sustained fracture. Bone, 2005, 36: 786–792
20 Veitch S W, Findlay S C, Hamer A J, et al. Changes in bone mass and bone turnover following tibial shaft fracture. Osteoporos Int, 2006, 17: 364–372
21 Stein G S, Lian J B. Molecular mechanisms mediating proliferation/differentiation interrelationships during progressive development of the osteoblast phenotype. Endocr Rev, 1993, 14: 424–442
22 Li H Z, Zhou Y, Guo G N. Effects of core binding facor α1 on promotion of osteoblastic differentiation from marrow mesenchymal stem cells. Zhongguo Xiufu Chongjian Waike Zazhi (in Chinese), 2006, 20: 121–124
23 Collin P, Nefussi J R, Wetterwald A, et al. Expression of collagen, osteocalcin, and bone alkaline phosphatase in a mineralizing rat osteoblastic cell culture. Calcif Tissue Int, 1992, 50: 175–183
24 Lazary A, Balla B, Kosa J P, et al. Effect of gypsum on proliferation and differentiation of MC3T3-E1 mouse osteoblastic cells. Biomaterials, 2007, 28: 393–399
25 Lipski A M, Pino C J, Haselton F R, et al. The effect of silica nanoparticle-modified surfaces on cell morphology, cytoskeletal organization and function. Biomaterials, 2008, 29: 3836–3846
26 Roux C, Cha F, Ollivier N, et al. Ti-Cp functionalization by deposition of organic/inorganic silica nanoparticles. Biomol Eng, 2007, 24: 549–554
27 Guehennec L L, Lopez-Heredia M A, Enkel B, et al. Osteoblastic cell behaviour on different titanium implant surfaces. Acta Biomaterialia, 2008, 4: 535–543
28 Zhang J C, Li X X, Xu S J, et al. Effect of the rare earth ions on proliferation, differentiation and function of osteoblasts in vitro. Prog Nat Sci (in Chinese), 2004, 14: 404–409
29 Taton T A. Nanotechnology: Boning up on biology. Nature, 2001, 412: 491–492
30 Ducy P, Zhang R, Geoffroy V, et al. Osf2/Cbfa1: A transcriptional activator of osteoblast differentiation. Cell, 1997, 89: 747–754
31 Nakashima K, Zhou X, Kunkel G, et al. The novel zinc finger-containing transcription factor osterix is required for osteoblast differentiation and bone formation. Cell, 2002, 108: 17–29
32 Yang S Y, Wei D Y, Wang D, et al. In vitro and in vivo synergistic interactions between the Runx2/Cbfa1 transcription factor and bone morphogenetic protein-2 in stimulating osteoblast differentiation. J Bone Miner Res, 2003, 18: 705–715
33 Beertsen W, Van Den Bos T. Alkaline phosphatase induces the deposition of calcified layers in relation to dentin: An in vitro study to mimic the formation of afibrillar acellular cementum. J Dent Res, 1991, 70: 176–181
34 Chou Y F, Dunn J C Y, Wu B M. In vitro response of MC3T3-E1 preosteoblasts within three-dimensional apatite-coated PLGA scaffolds. J Biomedic Mater Res, 2005, 75B: 81–90
35 Komori T, Yagi H, Nomura S, et al. Targeted disruption of Cbfa1 results in a complete lack of bone formation owing to maturational arrest of osteoblasts. Cell, 1997, 89: 755–764
36 Lee M H, Kim Y J, Kim H J, et al. BMP-2-induced Runx2 expression is mediated by Dlx5, and TGF-β1 opposes the BMP-2-induced osteoblast differentiation by suppression of Dlx5 expression. J Biol Chem, 2003, 278: 34387–34394
37 Pioletti D P, Takei H, Kwon Sym Wood D, et al. The cytotoxic effect of titanium particles phagocytosed by osteoblasts. J Biomed Mater Res, 1999, 46: 399–407
38 Kwon S Y, Takei H, Pioletti D P, et al. Titanium particles inhibit osteoblast adhesion to fibronectin-coated substrates. J Orthop Res, 2000, 18: 203–211
39 Martinez M E, Medina S, del Campo M T, et al. Effect of polyethylene particles on human osteoblastic cell growth. Biomaterials, 1998, 19: 183–187
40 Allen M J, Myer B J, Millett P J, et al. The effects of particulate cobalt, chromium and cobalt-chromium alloy on human osteoblast-like cells in vitro. J Bone Joint Surg Br, 1997, 79: 475–482
41 Jiang W, Kim B Y S, Rutka J T, et al. Nanoparticle-mediated cellular response is size-dependent. Nat Nanotechnol, 2008, 3: 145–150
42 Gutwein L G, Webster T J. Increased viable osteoblast density in the presence of nanophase compared to conventional alumina and titania particles. Biomaterials, 2004, 25: 4175–4183